Research Article

Journal of RAMAN SPECTROSCOPY

Received: 14 September 2009 Accepted: 7 February 2010 Published online in Wiley Online Library: 26 March 2010

(wileyonlinelibrary.com) DOI 10.1002/jrs.2646

Raman spectroscopic discrimination of pigments and tempera paint model samples by principal component analysis on first-derivative spectra†

Natalia Navas,[a]* Julia Romero-Pastor,[b] Eloisa Manzano[a] and Carolina Cardell[b]

This work explores the application of principal component analysis (PCA) on first-derivative Raman spectra to investigate historical tempera paint model samples. Various paint model samples were prepared containing pure blue pigments (azurite, lapis lazuli and smalt), pure red pigments (cinnabar, minium and raw Sienna), pure white pigments (lead white, chalk and gypsum), pure egg yolk as binder and tempera model samples obtained by mixing each of the pigments with the binder, and further characterized by Raman spectroscopy. The corresponding Raman spectra were used to apply PCA in order to test whether spectral differences allowed discrimination of samples based on their composition. Multivariate analyses were performed separately on three data matrices, one for each color, namely, white, blue and red, corresponding to the model samples, and all containing the spectral data of the binder model sample. Different pretreatments, that is log and derivative spectra, were performed on the spectra since no pattern distributions were obtained when the original Raman spectra were analyzed. Nevertheless, the multivariate analysis of the original Raman spectra was able to track alterations of sensitive pigments due to laser interaction. Results showed the excellent ability of PCA, when applied to the derived Raman spectra, to discriminate model samples according to their differing compositions in the three groups of model samples tested. This is the first attempt to use this approach in the field of cultural heritage and demonstrates the potential benefits for identifying historical pigments and binders for purposes of conservation and restoration.

Keywords: historical painting; micro-Raman spectroscopy; principal component analysis; first-derivative spectra

Introduction

At present, Raman microscopy (RM) is considered a well-established analytical technique to characterize artworks and their degradation products, providing valuable data for diagnostic information, preservation and restoration of artistic objects.[1] In fact, RM has become one of the most widely used techniques to study painting materials both organic (varnishes, binders and dyes)[2–4] and inorganic (pigments and extenders).[5–8] This is due to the high spatial resolution and accuracy of RM, which in addition provides rapid, reliable and specific results regarding both inorganic and organic components in the same sample.[9,10]

Ancient paintings are complex, composite materials made up of heterogeneous mixtures of organic and inorganic components.[11–13] Thus, Raman spectral interpretation of these materials can be a challenging task. Most previous studies on characterization of model and historical paintings are based on separate and independent analyses of the different painting components, because of sample complexity.[5–8] In fact, problems arise when the identification of individual components (pigments or binders) in mixtures is attempted[14] since few studies have addressed both binders and pigments simultaneously.[9,10] To solve this problem, mathematical methods are applied to facilitate the study of the spectral contributions from different components of a mixture.[14–17]

The development of mathematical operations on spectra such as derivatives is a well-known procedure. In the case of Raman spectroscopy, the use of second derivatives to reduce the fluorescence in the spectra is frequent,[18,19] although this method has the limitation of reducing band sensitivity. First-derivative Raman spectra followed by principal component regression was also proposed for multivariate calibration of coating thickness in pharmaceutical tablets.[20] Micro-Raman spectroscopy, combined with several chemometric techniques, has also been applied to differentiate between synthetic and natural indigo samples.[21] In this last work, the best discrimination of the samples was obtained by principal component analysis (PCA) before applying linear discriminant analysis to the second-derivative Raman spectra. PCA on Raman spectra was also used for the study of ceramics and glasses, but cluster variation approaches appeared to be

* *Correspondence to: Natalia Navas, Department of Analytical Chemistry, University of Granada, Fuentenueva s/n, 18071 Granada, Spain. E-mail: natalia@ugr.es*

† *Paper published as part of the Art and Archaeology 2009 special issue.*

a *Department of Analytical Chemistry, University of Granada, 18071 Granada, Spain*

b *Department of Mineralogy and Petrology, University of Granada, 18071 Granada, Spain*

Journal of RAMAN SPECTROSCOPY

more efficient.[22] However, to the authors' knowledge the use of first-derivative Raman spectra with PCA has not been reported in the study of complex, ancient painting materials.

In recent years, chemometric techniques have been used increasingly in the field of cultural heritage since they can extract information from correlated data, such as spectroscopic sets.[23] Nowadays, chemometric evaluation of spectral data is well accepted as a powerful tool for different purposes, including sample identification and recognition.[24] Among the different chemometric tools, PCA is a powerful data-mining technique that reduces data dimensionality and provides a more interpretable representation of the system under investigation.[25,26] In addition, valuable information is also obtained about the most important variables involved in the process of interest. The benefits of applying combined diffuse reflectance infrared Fourier transform spectroscopy (DRIFTS) and PCA for identifying historical pigments and binders were highlighted recently.[16] A similar approach using Fourier transform infrared spectral data was applied to study the UV ageing process of proteinaceous paint binder.[17] The principles of quality control and multivariate statistical analysis of Raman spectral data were successfully applied to monitor the conservation state of pigmented and wooden works of arts.[27,28] PCA on the Raman spectra of proteinaceous materials used in paints proved to be a powerful tool to discriminate among protein media on the basis of their Raman spectra,[29] as well as among naturally and artificially aged protein-based paint media.[15] In brief, all of these works demonstrate the increasing importance of multivariate analytical methods in the field of cultural heritage and a new trend in confronting problems related with works of art.

This paper explores the innovation of applying PCA on first-derivative Raman spectra to investigate model tempera paint samples. Thanks to the study of various paint model samples that contain pure blue pigments (azurite, lapis lazuli and smalt), pure red pigments (cinnabar, minium and raw Sienna), pure white pigments (lead white, chalk and gypsum), pure egg yolk as binder and mixtures of each of the pigments with the binder (tempera samples), different aspects of the benefits of this novel analytical approach are highlighted. The PCA-on-derivative Raman spectra approach to discriminate model samples based on its composition is described throughout this work.

Experimental

Painting materials

For this work, three blue pigments (azurite, lapis lazuli and smalt), three red pigments (cinnabar, minium and raw Sienna), and three white pigments (lead white, chalk and gypsum) were selected for analysis. Pigments were chosen on the basis of their widespread use throughout history. The azurite and smalt pigments were purchased from Kremer Pigments GmbH & Co. KG (Madrid, Spain). The rest of the pigments were supplied by Caremi Pigmentos (Sevilla, Spain).

Azurite is the hydrated copper carbonate $Cu_3(CO_3)_2(OH)_2$, and was the most important pigment in European paintings until the later part of the 17th century.[30] Lapis lazuli is a pigment made by grinding the semiprecious rock lapis lazuli whose main constituent is lazurite (Na_8-$10Al_6Si_6O_{24}S_{2-4}$). A famous and expensive pigment used since the 6th century A.D. in Afghan temples, it was worth more than gold during the Renaissance.[31] Smalt is an artificial pigment made of coarsely ground potassium cobalt glass strongly colored with cobalt oxide, which became a substitute for azurite and lapis lazuli in the 17th century.[32]

Regarding the red pigments, cinnabar is mercuric sulfide (HgS) and widely used in antiquity (e.g. 2nd millennium B.C. in China and since Neolithic period in Europe[33]) and still in use, despite its toxicity.[30] Minium is red oxide of lead (Pb_3O_4), also highly poisonous and one of the earliest pigments artificially prepared and still in use today.[34] Sienna and natural red earths represent a large group of clay-rich materials having a complex composition (e.g. gypsum, anhydrite, quartz, calcite, dolomite, etc.). The main coloring agents are either some nonclay pigment, for example iron oxides (haematite, goethite, magnetite, manganese oxides, etc.) or a chromogenous element in the clay structure.[35] The original pigment was obtained from Siena in Italy, from which the term is adopted.[36]

Lead white or ceruse is the chemical compound $(PbCO_3)_2{\cdot}Pb(OH)_2$; one of the oldest manmade pigments, it dates back to the ancient Egyptians and Greeks. Lead white was the principal white of classical European oil paintings.[37] Chalk is a natural white pigment made of calcium carbonate ($CaCO_3$), mainly used for painting grounds and in *fresco* paintings.[30] Natural gypsum ($CaSO_4{\cdot}2H_2O$) has been used in all forms since the beginning of civilization for artistic purposes.[38] In paintings, it has been traditionally used in ground layers and as filler or extender similar to chalk.

The protein binder selected was natural egg yolk, which has been used since ancient times. It solidifies quickly and is favorably flexible, but remains soft for long time and resists mechanical abrasion.[39]

Model samples

Nineteen model paint samples were prepared according to 'Old Master recipes' to obtain egg yolk tempera painting standards similar to those used by medieval artists.[40] Tempera is a painting technique in which finely ground pigments are first mixed with water and later blended with a solidifying proteinaceous binding agent, such as egg, animal glue or casein.[41] The first 9 model samples were pure pigments and the 10th the pure egg yolk binder. The nine remaining model samples were paint binary mixture samples composed by each of the pure pigments mixed with the egg yolk binder.

To prepare the binder, the egg yolk was separated from the white by the usual method of pouring it back and forth in the half shells. It was then rolled onto a paper tissue to remove the layer of clinging egg white and most of the chalazae. The skin was punctured at the bottom by a pin and the liquid content poured into a jar.[39]

The preparation of the tempera model samples was as follows: approximately 0.5 g of each pigment powder was formed as a crater-shaped mass and several drops of beaten egg yolk (different amounts according to each pigment) were added to form a fluid paste. This procedure was adapted to emulate real paint layers with variable pigment concentrations as found in ancient paintings. Then, one layer of the obtained paste was spread with a paintbrush to a fine coat on a glass slide. To obtain the pure binder model sample, the beaten egg yolk was directly spread onto the glass slide. By contrast, the pure pigment samples did not require this preparation, so the Raman measurements were done directly on the pigment powder.

Raman technique

A Renishaw Invia Raman microscope system fitted with a Peltier-cooled CCD detector and a Leica DMLM microscope was

Table 1. Specific working conditions for each analyzed sample

Samples	Laser (%)	Objective	Exposure time (s)	Accumulation (number)	Wavenumber (cm^{-1})
Binder					
Egg yolk	100	20	13	3	300–3800
White pigments					
Lead white	100	20	15	10	250–1600
Chalk	100	20	15	10	250–1200
Gypsum	100	20	15	5	350–1250
Lead white–egg	100	20	15	5	300–3500
Chalk–egg	100	20	15	5	250–3400
Gypsum–egg	100	50	10	5	350–3400
Blue pigments					
Lapis lazuli	25	20	10	5	200–1200
Smalt	100	50	10	10	200–1200
Azurite	1	50	10	10	200–1650
Lapis–egg	50	50	10	10	300–3400
Smalt–egg	100	50	10	5	200–3400
Azurite–egg	100	50	20	7	200–3400
Red pigments					
Cinnabar	1	20	10	10	200–450
Minium	5	50	10	5	100–600
Raw sienna	20	50	10	10	200–500
Cinnabar–egg	15	20	10	7	200–3400
Minium–egg	25	50	20	1	200–3400
Raw sienna–egg	25	50	10	10	200–3400

used. Samples were excited with the 514.5-nm line of an Ar laser (Laser Physics, model 23S514), with an average spectral resolution of approximately 1 cm^{-1} over the wavenumber range of 3800–200 cm^{-1}. To improve signal/noise ratios, spectra from 20-s exposure were averaged (n = 10). The spectra were recorded by placing the samples on the microscope stage and observing them with t long-working-distance 20× and 50× objectives. The sampled areas were identified and focused using either a video camera or microscope binoculars. Precautions were taken not to cause any damage to the samples (i.e. laser-induced degradation of paint materials). This was done by reducing the laser intensity and visually confirming the absence of damage in the sampling area with the help of the camera. Thus, laser power was kept between 0.2 and 20 mW. Moreover to avoid sample alteration and to obtain the best sample spectrum, we varied the laser power (% of 20 mW maximum), the number of spectra accumulations and irradiation exposure times for the diverse samples, as shown in Table 1.

Every sample was characterized by ten spectra obtained from the same location on the model sample in order to avoid spatial variation. The egg yolk model samples were characterized by 20 Raman spectra. Raman signals were collected by the probe and transferred via fiber optics to the CCD detector (NIR-enhanced), controlled by the Wire 2.0 software running on a personal computer.

Principal component analysis

PCA was performed separately on Raman spectral data on the basis of the color of the model samples, that is white, blue or red model samples. Three data matrices were built, one for each color, which initially included the spectra of the tempera model samples (30 spectra), the pure pigment model samples (30 spectra) and the pure egg yolk binder model samples (20 spectra). In this way, each color matrix was initially formed by 90 spectra. The principal components (PCs) were obtained using both the covariance data matrices (scaling by mean-centered data) and the correlation data matrixes (scaling by unit variance). Similar to previous works,[16,17] results were better when PCA was performed on correlation data matrices, so the results shown and discussed here correspond to autoscaled data. A simple centering data procedure is often adopted for spectral data[42,43] because the commonly applied autoscaling procedure assigns the same relevance to each spectral region. Thus spectral regions with small variation – no relevant bands – can acquire the same importance as large bands related to important functional groups. This problem was avoided in this work because only regions containing relevant bands were selected to apply PCA. These spectral regions were selected on the basis of the presence of characteristic bands of the pigments contained in the pigment-laden samples. The best results were obtained for the spectral regions shown in Table 2. Pretreatment techniques – log and first-derivative Raman spectra – were performed on the original Raman spectra before extracting the PCs. Log spectra were calculated using Excel 2000 (Microsoft Corporation, USA). First-derivative spectra were obtained using Spectrum Viewer 2.1b freeware program. PCA was performed using the Statistical Product and Service Solutions program (SPSS, for Windows ver. 15, USA).

Results and Discussion

The chemometric method PCA was applied in order to differentiate model samples on the basis of their different compositions.

Journal of RAMAN SPECTROSCOPY

Table 2. PCA results

Data matrix	Raman spectral region (cm^{-1})	PC	Variance account (%)	Variance accumulated (%)
White model samples	1200–600	PC1	65.3	65.3
		PC2	12.2	77.6
		PC3	6.1	83.7
		PC4	2.7	86.4
Blue model samples	1100–600	PC1	42.0	42.0
		PC2	26.5	68.5
		PC3	21.1	89.6
		PC4	1.6	91.2
Red model samples	1700–200	PC1	52.2	52.2
		PC2	12.0	64.2
		PC3	5.8	70.0
		PC4	2.6	72.6

First, this analysis was performed directly on the recorded Raman spectra separately for each color, that is white model samples, blue model samples and red model samples. Different Raman spectral regions were tested, including those with information on the pigments and also those at shorter Raman shifts, since no signal from the pigments appears at longer Raman shifts. Results from these multivariate analyses were discarded since they were uninformative for the three kinds of color model samples studied and for the different spectral regions tested. No pattern distributions were detected when projecting the samples onto the space of the firsts PCs, and the score plots showed no relation between sample distribution and composition for all the three color samples studied. No meaningful distribution could be assigned to the graphs. This meant that PCA was not able to detect differences in the recorded Raman spectra on the basis of the different composition of the samples.

Thus, in order to discern variability in the original Raman spectra, two pretreatments were performed on the spectral data matrices before extracting the PCs. These pretreatments were the logarithm and derivative of the recorded Raman spectra. No improvements were observed when applying PCA to the log-Raman spectra, which again produced uninformative score plots for the model samples. By contrast, however, when first-derivative spectra were used, the results indicated successful discrimination of the samples based on their different compositions for the three kinds of color model samples (white, blue and red). Consequently, all of the results presented and discussed in the remainder of this paper correspond to first-derivative Raman spectra. The transformation of a single Raman spectral band into its maximum and minimum, by calculating the first derivative of the spectra, apparently modifies the structure of the data matrix in such a way that differences are evident when PCA is applied. Small spectral differences in the original Raman spectra are seen in the first-derivative spectra, making possible PCA discrimination among samples based on their different composition.

White model samples

PCA was performed on several spectral regions that contained characteristic spectral bands of the white pigments. The highest quality information was obtained using the spectral region in the Raman shift interval 1100–600 cm^{-1}. The main spectral bands of the three pigments are found in this interval, that is at 1057 cm^{-1} for lead white, at 1086 cm^{-1} for chalk and at 1007 cm^{-1} for gypsum. PCA in the interval 1100–600 cm^{-1} allowed separation of the model samples according to their composition. The score plot of the first two PCs shown in Fig. 1(a) reveals that the first-derivative Raman spectral characteristics of this region exhibited enough difference to cluster the samples on the basis of their different chemical compositions. The results of the corresponding PCA in terms of explained variance (%) and cumulative explained variance (%) are shown in Table 2. An in-depth examination of the score plot of these two first PCs, which accounted for 77.6% of the total variance, reveals that the lead white samples clearly differ from the rest of the samples, the first PC being sufficient to discriminate them from the rest of the samples. Similarly, the pure gypsum samples were discriminated via the second PC. The rest of the samples were discriminated using both PCs. The scores of the pure chalk samples were identical; thus they clustered in the space of the two first PCs, near the gypsum tempera samples. Although these two types of samples were placed into the same cluster, there were small derivative spectral differences between them that allowed their separation. Surprisingly, the score plot of PC2 and PC4, which accounted only for 15.0% of the total variance, improved the results, and samples were better discriminated despite the fact that PC4 accounted only for 2.7% of the total variance (Fig. 1(b)).

The loading values indicate the specific contribution of each Raman shift in the calculation of the total variance of the derivative spectral data. Therefore, the loading plot can identify those Raman shift intervals that are important in the PC. A closer examination of the loading plots combined with the score plots can also reveal the kind of contribution associated with the PC. Since the scores of PC1 and PC2 discriminated lead white samples and gypsum samples, respectively, it is clear that the derivative spectral data variances due to these samples are mainly described by these PCs. Nevertheless, the interpretation of the loading plots is difficult since they did not directly represent the Raman spectrum, but rather its derivative. For example, a zero loading value corresponds to either a maximum or a minimum (zero first derivative) in the Raman spectrum.

Taking this into account, the contribution of each of the three white pigments is observed in the PC1 loading plot. A maximum and a minimum centered at zero for the Raman shift, corresponding to the characteristic Raman band of each pigment, was detected as shown in Fig. 1(c). The PC2 loading plot clearly indicates the contribution of the gypsum-laden samples in this PC because of the presence of a maximum and a minimum corresponding to its characteristic Raman band, that is 1007 cm^{-1} (Fig. 1(d)). Finally, from the loading plot of PC4, the Raman shift around 1086 cm^{-1} (maximum of chalk), 811 and 717 cm^{-1} weighs more heavily on this PC (Fig. 1(e)). The score plot in the spaces of PC4 and PC2 allowed a complete discrimination of the samples based on their composition (Fig. 1(b)). The use of the PC3 to build the score plots did not improve the results, and so is not discussed.

Blue model samples

The best capability to discriminate among the model samples by PCA was found in the Raman spectral shift between 1100 and 600 cm^{-1}. The main band of the Raman spectrum of the azurite pigment (401 cm^{-1}) was not included in this spectral region, nor

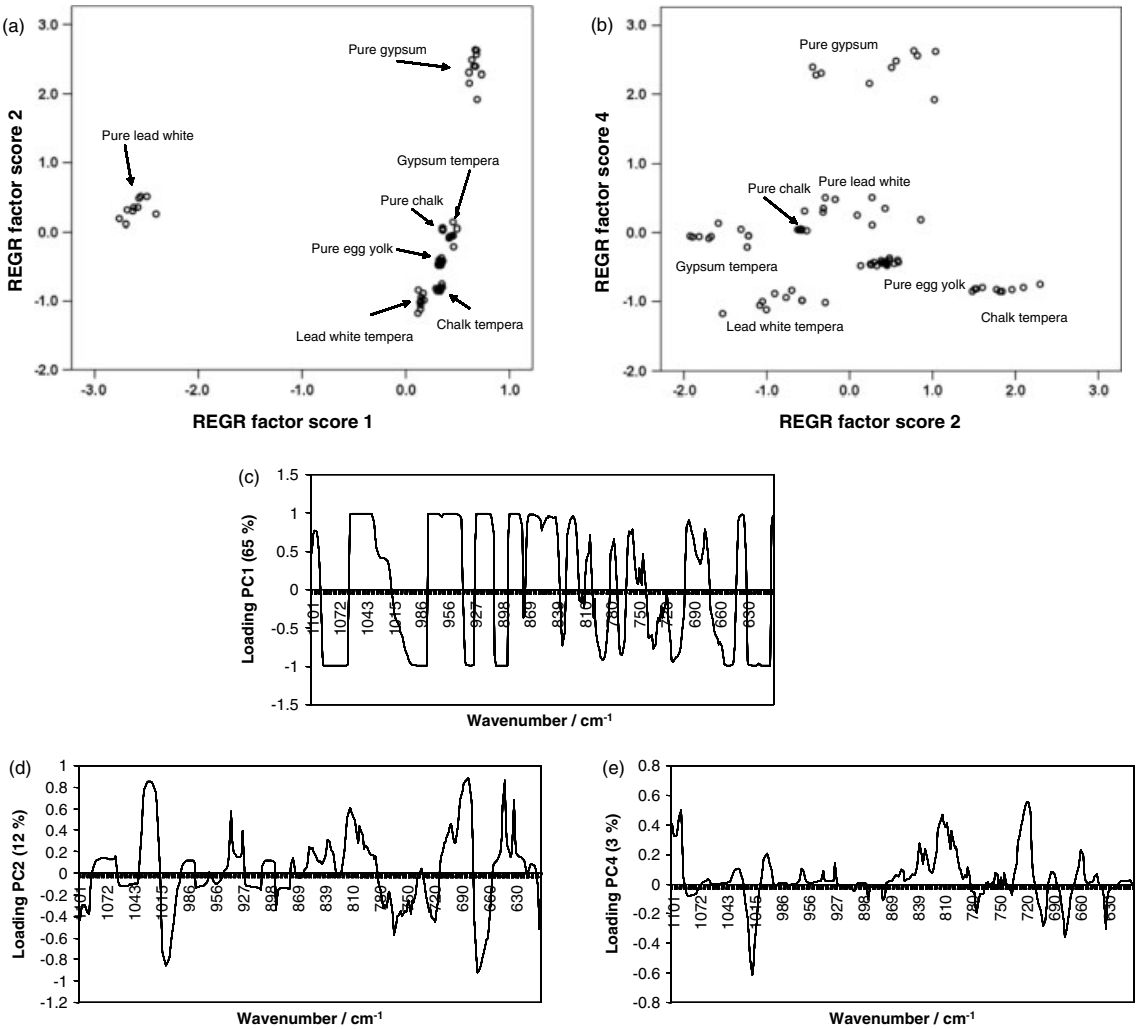

Figure 1. White model samples: (a) score plot of PC1 and PC2; (b) score plot of PC2 and PC4; (c) loading plot of PC1; (d) loading plot of PC2; (e) and loading plot of PC4.

was the main band of smalt (462 cm^{-1}). Bands at 761, 839, 933 and 1094 cm^{-1} were included; all these bands exhibited similar intensities. Also, for lapis lazuli its main spectral band was outside this spectral region (547 cm^{-1}). The spectral bands at 670, 802 and 1095 cm^{-1} were included, the latter having the highest intensity. The result of performing PCA on this spectral region is shown in Table 2. The first three PCs accounted for 89% of the total variance of the original Raman spectra studied (Table 2). The projection of the samples onto the spaces of the two first PCs, explaining 68% of the total variance, is shown in Fig. 2(a). This score plot shows the distribution of the samples in six groups based on the composition. Although the azurite model samples grouped near the smalt model samples in both Fig. 2(a) and (b), they did not cluster together in both score plots; rather, PC3 allowed slight separation of the azurite from the pure smalt (more negative scores).

Again, the interpretation of the information related to each PC was difficult since many spectral regions weighted the PCs as can be observed from the loading plots in Fig. 2(c)–(e). The analysis of the loadings of the first PC revealed that the spectral regions 1068–1009, 879–792 and 770–670 cm^{-1} had large positive values (Fig. 2(c)). Analysis of the derivative spectra of the model samples suggested that the first mentioned region could be related to the presence of egg yolk in the sample since its higher derivative band was located between 1045 and 929 cm^{-1}. The combination of the binder with the pigment could introduce small spectral changes in this region detected by the PCA, thus contributing to the discrimination of the samples. The most negative score value on PC1 was found for the azurite tempera model samples and the most positive value was for lapis lazuli tempera model samples, while the rest of the samples were characterized with score values near zero. The second and third regions could be related to the presence of the azurite pigment because its main derivative bands were located in this spectral region, that is between 863 and 718 cm^{-1}; nevertheless, the azurite tempera model samples had the most negative values. This result could be attributed to a significant change in the derivative spectra of the tempera with respect to those of the pure components (Fig. 2(c)). The second and third PCs also showed that the spectral region between 1092 and 1009 cm^{-1} gave large positive values (Fig. 2(d) and (c)). The score values of the tempera samples were positive on PC2, whereas those for pure pigment samples and egg yolk samples were negative. No improvement was found when using PC3 to project the samples (Fig. 2(b)).

Journal of RAMAN SPECTROSCOPY

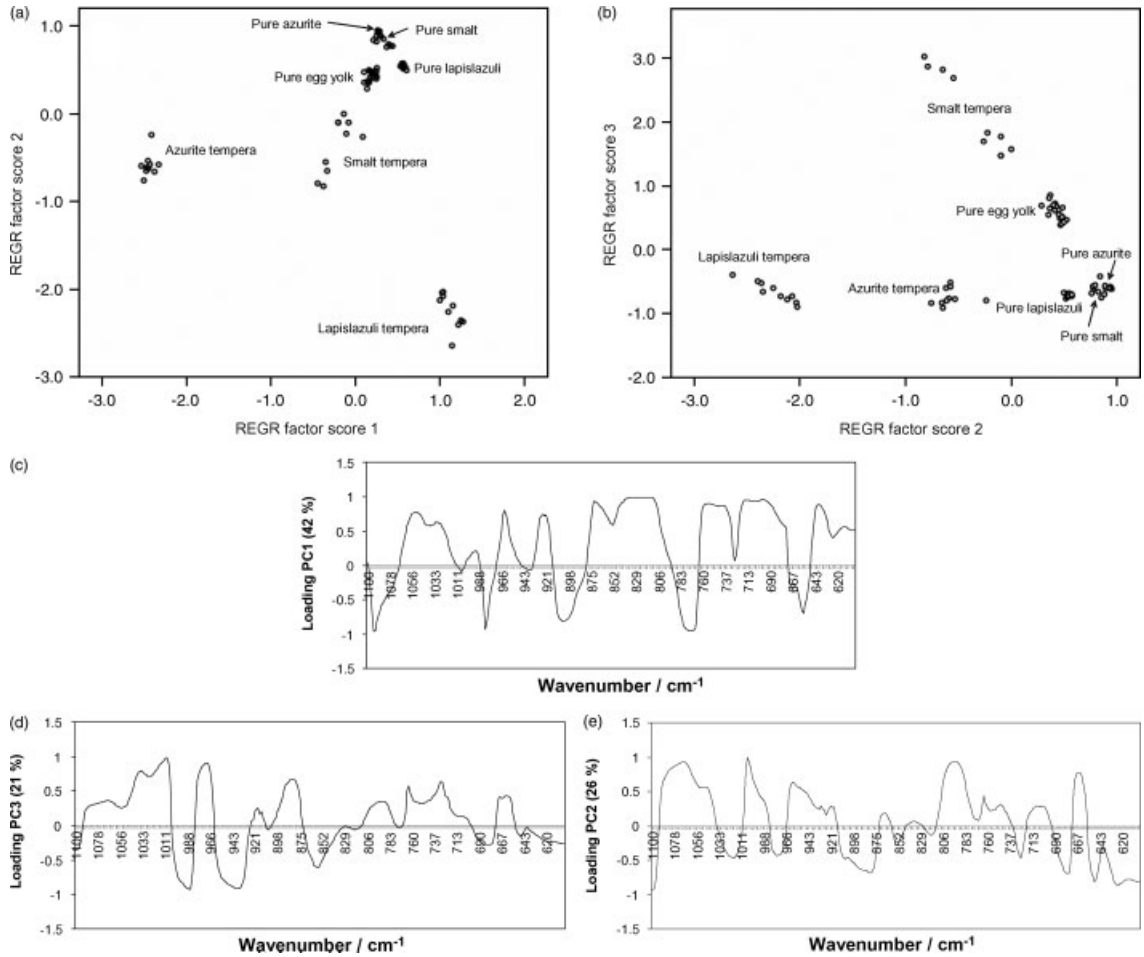

Figure 2. Blue model samples: (a) score plot of PC1 and PC2; (b) score plot of PC2 and PC3; (c) loading plot of PC1; (d) loading plot of PC3; (e) and loading plot of PC2.

Red model samples

Visual inspection of the minium Raman spectra and PCA (Fig. 3) revealed degradation of the minium samples by laser irradiation, in agreement with Burgio *et al.*[44] Consistent with the findings of these authors, minium degraded immediately when irradiated with the 514.5-nm excitation lines at any power, yielding a spectrum similar to that of massicot (orthorhombic PbO), with the main band at ~277 cm^{-1}. This degradation was detected only in the pure minium model samples, indicating protection of the pigment when mixed with the binder in its egg yolk tempera. The red model samples spectral differences were better discriminated when performing PCA on the Raman spectral data between 1700 and 200 cm^{-1} using centered data, where multiplicative effects were not eliminated. The score plot of the two PCs (Fig. 4(b)) accounting for 60.4% of the total variance, PC1 (41.7%) and PC2 (18.7%), shows a clear shift of the score distribution for the pure minium model sample, from the highest PC2 value for the first recorded Raman spectra to the much lower value for the last one. Thus, the degradation process of minium was mainly related to variance explained by PC2. PC1 mainly accounts for the discrimination of the egg yolk samples (positive values) from the rest of the samples containing pigments (negative values). From the score of the minium egg tempera grouped with the samples containing pigments, we infer that the egg yolk binder protected it from the degradation induced by the laser. Thus, this fact highlighted the capacity of PCA to track different degradation processes that may occur in pictorial samples by using Raman spectroscopic data.

In order to discriminate red samples on the basis of their composition, all the minium-laden samples were discarded from the original (recorded) and derivative spectral data matrixes. Thus, PCA was performed on data matrices with 60 spectra. As cited above, the best results were obtained when the derivative data matrix was used to apply PCA and the following results were obtained.

Again, different Raman shift intervals were tested for applying PCA. The highest quality information for discerning samples was obtained using the interval between and 1700 and 200 cm^{-1}. This includes the main Raman bands for the red pigments (at 251 and 343 cm^{-1} for cinnabar; at 214, 279 and 394 cm^{-1} for raw Sienna), and several characteristic Raman bands for the egg yolk (at 1156, 1440 and 1524 cm^{-1}). The results of the PCA are summarized in Table 2. Projection of the data samples from the original space into the plane of the two first PCs, explaining 64.2% of the total variance, is shown in Fig. 4(a). Three clear groups are distinguished. The first PC must be related to the presence of pigment in the model samples. The samples were divided in two groups in this PC, which score positive for the egg yolk model samples and negative for the rest of the model samples (each with a pigment in the composition), and gave negative score values.

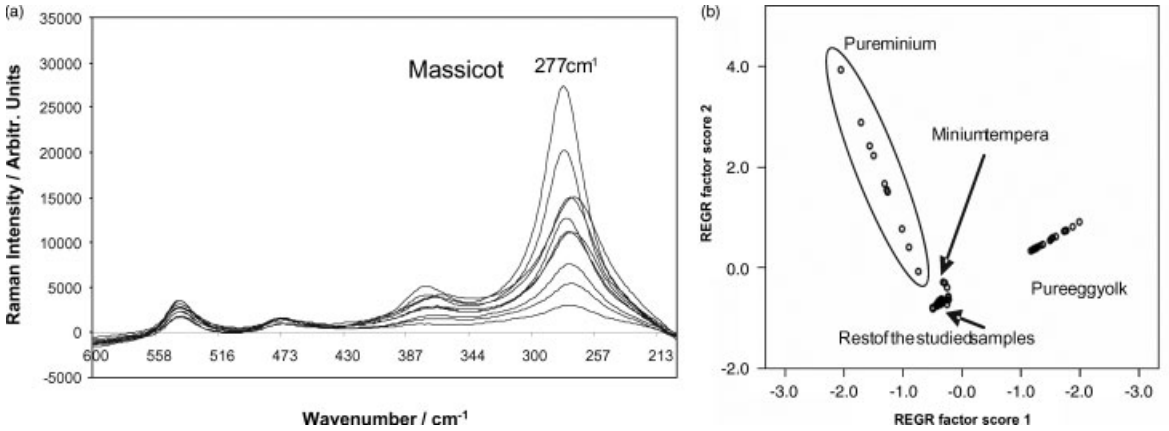

Figure 3. Minium degradation process: (a) spectra of massicot (277 cm^{-1}) obtained after irradiating minium with the Ar laser (514.5 nm); (b) score plot of the two principal components, PC1 and PC2. Raman spectra of all the red model samples were included in the PCA using centered data.

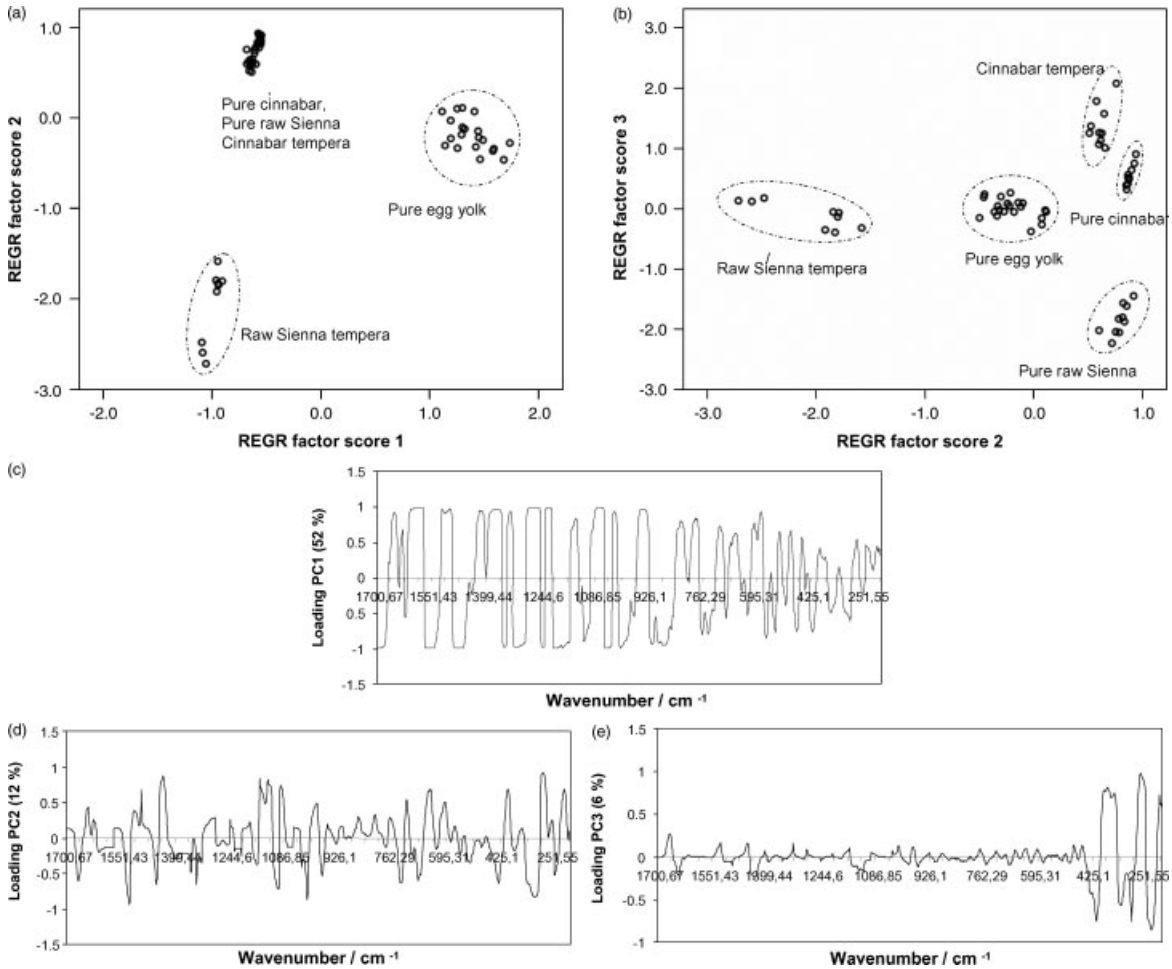

Figure 4. Red model samples: (a) score plot of PC1 and PC2; (b) score plot of PC2 and PC3; (c) loading plot of PC1; (d) loading plot of PC2; (e) and loading plot of PC3.

Loading plot for PC1 indicated that the whole spectral interval selected contributed to the score value, and thus the whole interval contributed to discriminate the presence of pigment in the model samples (Fig. 4(c)). In PC2, raw Sienna tempera model samples were separated from the rest of the studied samples by negative score values. Loading plot of this PC again indicated a contribution of the whole spectral interval in grouping the samples (Fig. 4(d)). Finally, the score plot of PC2 and PC3 grouped samples according to their composition as shown in Fig. 4(b). Five groups could be clearly discriminated, one for each type of model sample. From the loading plot of PC3, it is clear that this component is mainly related to the sample pigment composition (Fig. 4(e)). The spectral region weighting this derivative PC corresponds to the bands of the pigments (between 430 and 200 cm^{-1}).

Conclusions

In this study, PCA of first-derivative Raman spectra of pure and tempera model paint samples has demonstrated its capability to discriminate samples on the basis of their composition. This approach provides a novel and complementary method for discerning among egg yolk temperas used in ancient paintings. Model samples prepared following Old Master recipes were analyzed by RM, showing the usefulness of this technique to study artistic materials like pigments and egg yolk binder. In addition, laser degradation of the red pigment minium was detected by multivariate analysis. To validate the analytical approach, the PCA was performed separately on the derivative spectra of white, blue and red model samples. In all cases, the approach proved a powerful tool to discriminate tempera samples on the basis of their composition, including tempera and pigment. In future work, it would be very interesting to extend such study to different binders and attempt the study of real samples.

Acknowledgements

Financial support for this work was provided by Spanish Science Ministry Projects BHA2003-08671 and HUM-2006-09262/ARTE, the Andalusian Research Group RNM-179, and a research contract from the *Junta de Andalucía* awarded to C. Cardell. We thank A. Yebra-Rodríguez for helping with Raman microscopy using equipment from the University of Jaén, and A. Kowalski for English revision.

References

[1] P. Baraldi, A. Tinti, *J. Raman Spectrosc.* **2008**, *35*, 963.
[2] P. Vandenabeele, B. Wehling, L. Moens, H. Edwards, M. De Reu, G. Van Hooydonk, *Anal. Chim. Acta* **2000**, *407*, 261.
[3] P. Vandenabeele, S. Bodé, S. A. Alonso, L. Moensa, *Spectrochim. Acta; Part A* **2005**, *61*, 2349.
[4] G. Burrafato, M. Calíbrese, A. Cosentino, A. M. Gueli, S. O. Troja, A. Zuccarello, *J. Raman Spectrosc.* **2004**, *35*, 879.
[5] P. Vandenabeele, L. Moens, *Compr. Anal. Chem.* **2004**, *42*, 635.
[6] I. M. Bell, R. J. H. Clark, P. J. Gibbs, *Spectrochim. Acta, Part A* **1997**, *53*, 2159.
[7] L. Burgio, R. J. H. Clark, *Spectrochim. Acta; Part A.* **2001**, *57*, 1491.
[8] R. J. H. Clack, *J. Mol. Struct.* **2007**, *74*, 834.
[9] M. Pérez-Alonso, K. Castro, J. M. Madariaga, *Anal. Chim. Acta.* **2006**, *571*, 121.
[10] P. Vandenabeele, K. Castro, M. Hargreaves, L. Moensa, J. M. Madariaga, H. G. M. Edwards, *Anal. Chim. Acta.* **2007**, *588*, 108.
[11] A. M. Correia, M. J. V. Oliveira, R. J. H. Clark, M. I. Ribeiro, M. L. Duarte, *Anal. Chem.* **2008**, *80*, 1482.
[12] C. Cardell, L. Rodriguez-Simón, I. Guerra, A. Sánchez-Navas, *Archaeometry* **2009**, *51*, 637.
[13] A. Andreotti, I. Bonaduce, M. P. Colombini, G. Gautier, F. Modugno, E. Ribechini, *Anal. Chem.* **2006**, *78*, 4490.
[14] M. Breitman, S. Ruiz-Moreno, A. López-Gil, *Spectrochim. Acta; Part A* **2007**, *68*, 1114.
[15] A. Nevin, D. Anglos, A. Burnstock, S. Cather, M. Becucci, C. Fotakis, E. Castellucci, *J. Raman Spectr.* **2008**, *39*, 307.
[16] N. Navas, J. Romero-Pastor, E. Manzano, C. Cardell, *Anal. Chim. Acta* **2008**, *630*, 141.
[17] E. Manzano, N. Navas, R. Checa-Moreno, L. Rodríguez-Simón, L. F. Capitán-Vallvey, *Talanta* **2009**, *77*, 1724.
[18] A. O'Grady, A. C. Dennis, D. Denvir, J. J. McGarvey, S. E. J. Bell, *Anal. Chem.* **2001**, *73*, 2058.
[19] T. L. Weis, Y. Jiang, E. R. Grant, *J. Raman Spectrosc.* **2004**, *35*, 813.
[20] J. F. Kauffman, M. Dellibovi, C. R. Cunninghamb, *J. Pharm. Biomed. Anal.* **2007**, *43*, 39.
[21] P. Vandenabeele, L. Moens, *Analyst* **2003**, *128*, 187.
[22] P. Colomban, A. Tournier, *J. Cult. Herit.* **2007**, *8*, 242.
[23] M. F. Musumarra, *Chemometr. Intell. Lab. Syst.* **1998**, *44*, 363.
[24] P. Geladi, B. Sethson, J. Nystroem, T. Lillhonga, T. Lestander, J. Burger, *Spectrochim. Acta B* **2004**, *59*, 1347.
[25] S. Wold, K. Esbensen, P. Geladi, *Chemom. Intell. Lab. Syst.* **1987**, *2*, 37.
[26] J. E. Jackson, *A User's Guide to Principal Components*, John Wiley & Sons, Inc.: New York: **1991**.
[27] E. Marengo, E. Robotti, M. C. Liparota, M. C. Gennaro, *Anal. Chem.* **2003**, *75*, 5567.
[28] E. Marengo, E. Robotti, M. C. Liparota, M. C. Gennaro, *Talanta* **2004**, *63*, 987.
[29] A. Nevin, L. Osticioli, D. Anglos, A. Burnstock, S. Cather, E. Castelluci, *Anal. Chem.* **2009**, *79*, 6143.
[30] N. Eastaugh, V. Walsh, T. Chaplin, R. Siddall, *Pigment Compendium: A Dictionary of Historical Pigments*, Butterworth-Heinemann: Oxford, **2004**.
[31] D. Marano, I. M. Catalana, A. Monno, *Spectrochim. Acta A.* **2006**, *64*, 1147.
[32] I. Borgia, B. Brunettia, I. Mariania, A. Sgamellottia, F. Cariati, P. Fermob, M. Mellinic, C. Vitic, G. Padelettid, *Appl. Surf. Sci.* **2002**, *185*, 206.
[33] U. B. Mioc, P. Colomban, G. Sagon, M. Stojanovic, R. Rosic, *J. Raman Spectrosc.* **2004**, *35*, 843.
[34] M. Matteini, M. Arcanuelo, *La Química en la Restauración*, Editorial Nerea: Sevilla, **2001**.
[35] F. Froment, A. Tournie, P. Colomban, *J. Raman Spectrosc.* **2008**, *39*, 560.
[36] D. Hradil, T. Grygara, J. Hradilova, P. Bezdicka, *Appl. Clay Sci.* **2003**, *22*, 223.
[37] D. A. Scott, S. Warmlander, J. Mazurek, S. Quirke, *J. Archaeol. Sci.* **2009**, *36*, 923.
[38] A. Heywood, in *The Use of Huntite as a White Pigment in Ancient Egypt. Colour and Painting in Ancient Egypt*, British Museum Press: London, **2001**, pp 5.
[39] R. Mayer, in *The Artists Handbook of Materials and Techniques* (Ed.: S. Sheehan), The Viking Press: New York, **1991**.
[40] F. Pacheco, *El arte de la Pintura*, Cátedra: Madrid, **1990**.
[41] L. Masschelein-Kleiner, *Ancient Binding Media; Varnishes and Adhesives*, ICCROM: Rome, **1995**.
[42] E. Marengo, M. C. Liparota, E. Robotti, M. Bobba, M. C. Gennaro, *Anal. Bional. Chem.* **2005**, *381*, 884.
[43] D. L. Massart, B. G. M. Vanderginste, L. M. C. Buydens, S. De Jong, P. J. Lewi, J. Smeyers-Verbeke, *Handbook of Chemometrics and Qualimetrics. Part A*, Elsevier: Amsterdan, **1997**.
[44] L. Burgio, R. J. H. Clark, S. Firth, *Analyst* **2001**, *126*, 222.

